Shear-Induced Disruption and Recovery of Microphase-Separated Network Structure of a BSB Triblock Copolymer in Dibutyl Phthalate

Hendra Tan,[†] Hiroshi Watanabe,*[,†] Yumi Matsumiya,[†] Toshiji Kanaya,[†] and Yoshiaki Takahashi[‡]

Institute for Chemical Research, Kyoto University, Uji, Kyoto 611-0011, Japan, and Department of Molecular & Materials Sciences, IGSES, Kyushu University, Fukuoka 812-8581, Japan

Received November 4, 2002; Revised Manuscript Received December 30, 2002

ABSTRACT: Rheological and structural properties were examined for a 30 wt % solution of a 1,4-butadiene−styrene−1,4-butadiene (BSB) triblock copolymer ($M_S = 108 \times 10^3$, $M_B = 13.3 \times 10^3$ for each B block) in an S-selective solvent, dibutyl phthalate (DBP). At equilibrium at 25 °C, a bcc lattice of the unsolved, soft (rubbery) B domains connected by the middle S blocks (a lattice-type network) was formed to exhibit the elastic behavior against small strains. This lattice-type network was disrupted under steady shear to lose its elasticity, and the strongest disruption occurred at an intermediate shear rate ($\dot{\gamma}$) close to a frequency of B/S concentration fluctuation. This disruption behavior was similar to that of a BS/DBP diblock micellar lattice system. However, for the BSB/DBP system, an order of magnitude increase of $\dot{\gamma}$ resulted in a minor change (by a factor <30%) of a time t_r^∞ required for the full recovery of the elasticity during a quiescent rest after the preshear. This result, quantitatively different from that seen for the BS/DBP diblock system, was related to the bridge-type configuration of the middle S blocks of BSB: Under the steady shear, a large fraction of the bridges in the flowing defect region would be converted into loops. Thus, the re-formation of the bridges in this region (a process absent in the BS/DBP system) should be required for the full recovery of the elasticity of the BSB/DBP system. This bridge re-formation, leading to a recovery of the order of the B domain arrangement and allowing the coexisting loops to exhibit the elasticity, should be accompanied by a transient mixing of the B and S block and thus gave the very weakly $\dot{\gamma}$-dependent t_r^∞ determined by the mixing enthalpy.

1. Introduction

B−A−B-type triblock copolymers behave as a thermoplastic elastomer in the microphase-separated state, and their rheological properties have been extensively investigated.[1−13] The properties change with various factors including the morphology (microdomain shape), the A/B segregation power, and the configurations of the middle A blocks.

In particular, the effect of the middle block configuration on the rheological properties is an important problem not existing for the B−A diblock copolymers: The middle A block of the microphase-separated B−A−B copolymer takes either the bridge or the loop configurations, and the end B blocks connected to the bridge-type middle block work as a physical anchor for this middle block. Under steady flow, the bridge pulls out its anchor from one B domain and transfers this anchor to the other domain, thereby converting itself into a new bridge and/or loop.[5−7] This anchor pulling-out process involves a transient, unfavorable mixing of the A and B blocks and is associated with an enthalpic barrier that provides the system with an elastoplastic feature.

The loop-type middle A blocks coexisting with the bridges also contribute to the elastoplastic feature when the B domains are *regularly arranged* on a cubic lattice.[8−10] For this case, neighboring A blocks have correlated conformations due to the osmotic (thermodynamic) requirement of uniform space filling, and an applied strain distorts the conformation of these blocks *even if they are in the dangling loop state*. This distortion results in the equilibrium elasticity of those osmotically correlated A loops under small strains.[8,9] This mechanism of the loop elasticity is similar to that of the elasticity observed for micellar lattices of B−A diblock copolymers. The micellar system includes no bridge-type chains, but the tail-type corona A blocks (similar to the loops) entropically sustain the elasticity when they are osmotically correlated with each other:[14−17] The equilibrium modulus G_e of the micellar lattice systems is proportional to the tail number density ν but is smaller than the modulus expected for *uncorrelated* entropic strands, $G_e° = \nu k_B T$ (k_B = Boltzmann constant and T = absolute temperature), reflecting the osmotic correlation of the neighboring tails.[17]

The elastoplasticity due to the bridges and loops has been observed for styrene−isoprene−styrene (SIS) triblock copolymers in an I-selective solvent, *n*-tetradecane.[8−10] Specifically, the loop fraction ϕ_l was dielectrically estimated for concentrated SIS copolymer chains having inverted parallel dipoles in the I blocks:[10] The ϕ_l increased from ≅60% up to ≅80% with decreasing SIS concentration from 50 to 20 wt %. Namely, the loop is the major configuration for those SIS chains. The bridge- and loop-type middle I blocks almost equally contribute to the equilibrium elasticity (under small strains) and the plasticity (under large strain/flow).[9,10]

Thus, the steady flow behavior of the microphase-separated triblock copolymers reflects the domain structures under the flow as well as the mechanical responses of both bridges and loops under an influence of the defects in the domain arrangement. (If the defects are aligned in the flow direction, the flow mainly occurs at the defects, thereby minimizing the flow-induced disruption of the domain arrangement.[17,18]) In relation to this flow behavior, it is of interest to examine the time-

[†] Kyoto University.
[‡] Kyushu University.
* To whom correspondence should be addressed.

10.1021/ma021654q CCC: $25.00
Published on Web 03/25/2003

dependent rheological changes of the triblock copolymer system during a rest after the steady shear. A large fraction of the bridges (in the flowing defect regime) would be converted into loops under the shear,[5−7] and the recovery of the equilibrium bridge population (bridge re-formation) during the rest is expected to affect those rheological changes.

From this point of view, we have examined the rheological/structural properties of a butadiene−styrene−butadiene (BSB) triblock copolymer dissolved in a moderately S-selective solvent, dibutyl phthalate (DBP). Small-angle neutron scattering (SANS) measurements revealed that a cubic lattice of the unsolved, soft (rubbery) B domains connected by the S bridges (a lattice-type network) was disrupted to various magnitudes under the steady shear at various rates. For this disrupted network, the recovery of the equilibrium elasticity during a quiescent rest was traced with time. The time required for the full recovery was found to change only weakly with the magnitude of the network disruption during the shear. This feature, being in contrast to that observed for a sheared micellar lattice of a BS copolymer in DBP,[19] was related to the re-formation of the flow-disrupted bridges, a process absent in the BS/DBP system. Details of these results are presented in this paper.

2. Experimental Section

2.1. Material. In the previous study,[19] a symmetric 1,4-butadiene−styrene−1,4-butadiene (BSB) triblock copolymer was obtained through a head-to-head coupling of BS^- precursor living anions and successive fractionation. This copolymer, having deuterated B and protonated S blocks, was fully characterized previously with GPC (equipped with refractive index and ultraviolet absorption detectors):[19] $M_S = 108 \times 10^3$, $M_B = 13.3 \times 10^3$ for each B block, and $M_w/M_n = 1.03$.

A system subjected to rheological and SANS measurements was a 30 wt % solution of the BSB copolymer dissolved in dibutyl phthalate (DBP), a moderately S-selective solvent.[20,21] For comparison, the rheological measurement was conducted also for a BSB/DBP solution having a little lower BSB concentration, $C_{BSB} = 29$ wt %. These solutions were prepared by uniformly dissolving prescribed masses of BSB and DBP in excess methylene chloride and then allowing methylene chloride to completely evaporate.

Under an assumption of no volume change on dissolution, the characteristic molecular weight for the entanglement of the BSB copolymer chains was evaluated to be $M_C \cong M_C^\circ/\varphi_{BSB} \cong 110 \times 10^3$ for $C_{BSB} = 29-30$ wt %, where M_C° ($= 32 \times 10^3$)[22] is the characteristic molecular weight for bulk S block (the major component in the copolymer) and φ_{BSB} is the volume fraction of the BSB chains in the solutions. This M_C is comparable with the M_{BSB} of the BSB chains, indicating that the chains were barely entangled in the solutions examined.

2.2. Measurements. For the BSB/DBP systems with $C_{BSB} = 29$ and 30 wt %, rheological measurements were carried out at 25 °C with a laboratory rheometer (ARES, Rheometrics). A cone-and-plate fixture with the plate diameter = 25.0 mm and the gap angle = 0.1 rad was used. In the dynamic measurements, the amplitude of the oscillatory strain was kept small ($\gamma_0 < 0.01$) to ensure the linearity of the measured storage and loss moduli, $G'(\omega)$ and $G''(\omega)$ with ω being the angular frequency.

The BSB/DBP systems charged in the rheometer were first disordered at 60 °C for 15 min, quiescently cooled to 25 °C, and then annealed at 25 °C for 16 h. After this annealing process, the 30 wt % system exhibited the elastic behavior against small strains at low ω. This elasticity resulted from a lattice-type network structure of the B domains connected by the S bridges, as revealed from SANS measurements. The 29 wt % system fully relaxed at low ω and exhibited no elasticity,

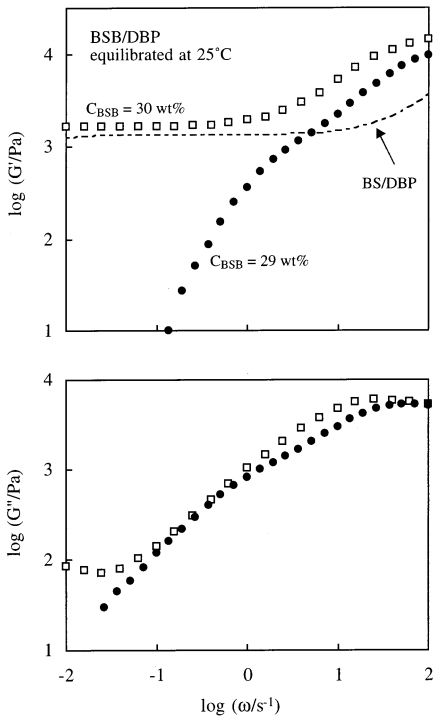

Figure 1. Linear viscoelastic moduli of the BSB/DBP systems ($C_{BSB} = 29$ and 30 wt %) equilibrated at 25 °C. The dotted curve indicates the storage modulus of the previously examined 28 wt % BS/DBP system.[19]

suggesting that the microphase separation concentration at 25 °C was just below $C_{BSB} = 30$ wt %.

For the 30 wt % BSB/DBP system equilibrated at 25 °C, the steady-state viscosity $\eta(\dot\gamma)$ was measured at various shear rates $\dot\gamma$. The lattice-type network formed at equilibrium was disrupted to various magnitudes according to the $\dot\gamma$ value, as confirmed from SANS measurements. Correspondingly, the G' at low ω measured immediately after the steady shear was significantly smaller than the equilibrium modulus. During the quiescent rest after the shear, linear viscoelastic measurements were made to trace changes (increases) of G' with the time t. This change reflected a recovery of the equilibrium network structure.

For the 30 wt % BSB/DBP system, the SANS measurements were made with the SANS-U spectrometer at the Neutron Scattering Laboratory, Institute for Solid State Physics, University of Tokyo (Tokai, Ibaragi), in the following configuration: incident neutron wavelength $\lambda = 0.7$ nm, wavelength spread $\Delta\lambda/\lambda = 0.1$, sample-to-detector distance = 4.00 m, and beam diameter = 0.3 cm. The scattering intensity was measured as a function of the scattering vector $\mathbf{q}$, where $q = |\mathbf{q}| = [4\pi/\lambda] \sin(\theta/2)$ with θ being the scattering angle. The measurements were made at 25 °C in a Couette flow cell[23] with inner and outer radii of 25.25 and 27.00 mm. The system was quiescently ordered in the cell (by cooling from 60 to 25 °C), and the SANS profiles were obtained at equilibrium and under steady shear. The incident beam was in the direction of the velocity gradient, and the profiles were detected in a velocity−vorticity plane. All SANS profiles were azimuthally symmetric within experimental resolutions, indicating that the lattice-type network was not significantly oriented (even under the shear). In this paper, we present the circularly averaged profiles $I(q)$ without a correction for the incoherent scattering.

3. Results and Discussion

3.1. Linear Viscoelastic Behavior and Structure at Equilibrium. For the 29 and 30 wt % BSB/DBP systems equilibrated at 25 °C, Figure 1 shows the ω dependence of the storage and loss moduli, G' and G''

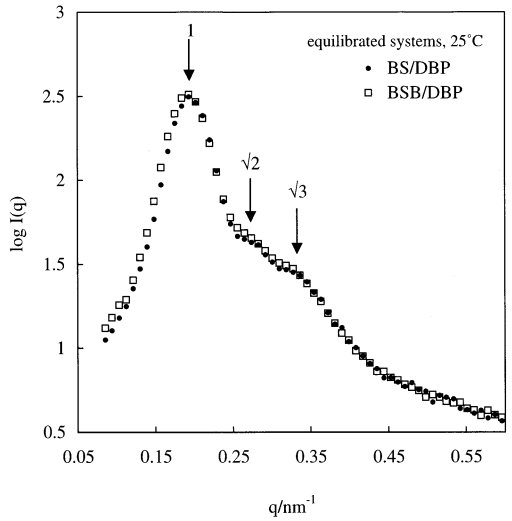

Figure 2. SANS profiles of the 30 wt % BSB/DBP and 28 wt % BS/DBP systems equilibrated at 25 °C.

(symbols). For comparison, the G' data of a previously examined BS/DBP system[19] (C_{BS} = 28 wt %) are also shown (dotted curve). This BS diblock copolymer is a half fragment (precursor) of the BSB triblock copolymer. Throughout this paper, we compare the rheological/structural properties of the BSB and BS systems to examine their similarity/difference.

As seen in Figure 1, the BSB systems exhibit a fast relaxation process (with a characteristic frequency $\omega_{chain} \cong 10\ s^{-1}$) attributable to the orientation relaxation of individual BSB chains.[19] More importantly, the full relaxation characterized with the terminal tails ($G' \propto \omega^2$ and $G'' \propto \omega$) is observed at low ω for C_{BSB} = 29 wt % while the elastic behavior characterized with the low-ω plateau of G' ($\gg G''$) is noted for C_{BSB} = 30 wt %. This result suggests that the microphase separation at 25 °C occurred at C_{BSB} between 29 and 30 wt %.

Concerning this elastic behavior, we also note a weak increase of G'' of the 30 wt % BSB system at the low-ω end of our experimental window. This increase suggests an existence of an extremely slow, partial relaxation process (with a characteristic frequency $\ll 0.01\ s^{-1}$).[24] However, in this paper, we limit ourselves in a range of $\omega \geq 0.01\ s^{-1}$ and utilize G' at $\omega = 0.01\ s^{-1}$ as the equilibrium modulus G_e.

Figure 2 shows the circularly averaged $I(q)$ profiles of the 30 wt % BSB/DBP and 28 wt % BS/DBP[19] systems equilibrated at 25 °C. (The scattering before this averaging was azimuthally symmetric.) These profiles, shown in a semilogarithmic scale (log I vs q), were obtained for the incident neutron beam of the same intensity over the same exposure time (10 min). For the BSB system, scattering peak/shoulders attributed to the interference between the spherical B domains (minor component not dissolved in DBP) are observed at q = 0.19, 0.27, and 0.33 nm^{-1}, confirming the microphase separation at C_{BSB} = 30 wt %. A ratio of these q values is close to a ratio for a bcc lattice, $1:\sqrt{2}:\sqrt{3}$ (see the arrows). Thus, the B domains form a bcc polycrystalline lattice and the neighboring B domains are connected by the S bridges coexisting with the S loops. This lattice-type network structure provides the 30 wt % BSB system with the equilibrium elasticity observed in Figure 1. (The q_1 value of the first-order scattering peak gives the cell edge length of the bcc lattice, $a \cong 47$ nm. From this a value and the M_{BSB} and C_{BSB} values, the B domain radius is evaluated to be ≅9.3 nm under an assumption of no swelling of the B domains with DBP.)

In Figure 2, we also note that the $I(q)$ profile is almost identical for the BSB/DBP and BS/DBP systems having nearly the same concentration (C_{BSB} = 30 wt % and C_{BS} = 28 wt %). This type of coincidence is well-known for a diblock copolymer and its head-to-head dimer[25] (e.g., BS and BSB). However, some comments need to be made for a close coincidence of the equilibrium moduli G_e of the BS and BSB systems (Figure 1).

The lattice of the diblock copolymer micelles is formed as a result of the osmotic constraint for the tail-type corona blocks:[14−17] Since these blocks are required to maintain a uniform concentration distribution in the solvated corona phase while keeping their conformations as random as possible, the micellar cores are forced to arrange themselves on a cubic lattice that is spatially symmetric and helpful for this uniform distribution to be achieved. The G_e of the BS/DBP system (cf. dotted curve in Figure 1) reflects the thermodynamic stability of this lattice sustained by the osmotically correlated corona S blocks.

Similarly, the lattice-type network of the spherical B domains in the BSB/DBP system is formed as a result of the osmotic constraint for the middle S blocks having either the bridge or loop configurations. For styrene−isoprene−styrene (SIS) triblock copolymers dissolved in an I-selective solvent, *n*-tetradecane (C14), the loop fraction increases up to ≅80% with decreasing C_{SIS} down to 20 wt %.[10] Namely, the loop is a major configuration in the system having a relatively small C_{SIS}. This should be the case also for our 30 wt % BSB/DBP system.

Here, we should emphasize that a dangling loop in the BSB/DBP system is elastically active under the osmotic constraint as long as the lattice-type network has a high regularity.[8,9] The dangling loop (as well as the knotted loop and bridge) is distorted by the applied strain so as to maintain the uniform concentration distribution, and this distortion results in the equilibrium elasticity of the loops. In fact, for nonentangled SIS/C14 systems, previous studies[9,10] demonstrated that the elasticity sustained by a loop is similar, in magnitude, to that sustained by a bridge. This loop elasticity is also similar to the tail elasticity observed for the SI micellar system. The close coincidence of G_e of the barely entangled BSB and BS systems (Figure 1) quite possibly reflects these similarities of the elasticity of the loop, bridge, and tail. (Note that the G_e of the BSB system should have been considerably smaller than G_e of the BS system *if* the loops, the major configuration in the former, were elastically inert.)

It should be also emphasized that the tail elasticity in the BS/DBP micellar system vanishes when the micellar lattice is disrupted under the shear:[19] The S concentration profile in the corona phase of the disrupted lattice should have a spatial gradient in the quiescent state (before the re-formation of the lattice), and an extra concentration gradient created by a small applied strain is not significant compared to the gradient already existing in that state. For this case, the S tails do not exhibit the osmotic restoring force (equilibrium elasticity) against the strain. Similarly, the loop-type S blocks in the BSB/DBP system would exhibit no elasticity when the cubic arrangement of the B domains is disrupted by the shear. This point becomes a key in

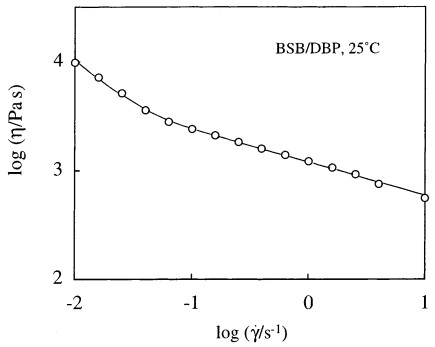

Figure 3. Steady-state viscosity of the 30 wt % BSB/DBP system at 25 °C.

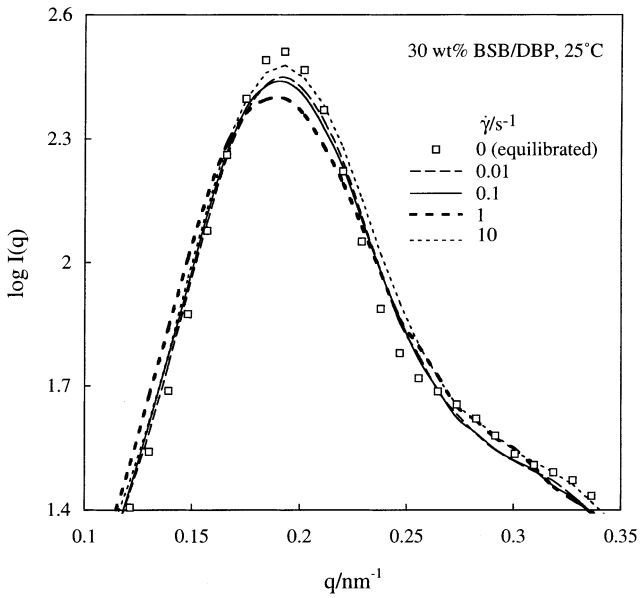

Figure 4. SANS profiles of the 30 wt % BSB/DBP system under steady shear (curves). The squares indicate the profile at equilibrium ($\dot{\gamma} = 0$).

our later discussion of the rheological changes of the BSB system after imposition of the steady shear.

3.2. Rheology and Structure under Steady Shear. Figure 3 shows the steady-state viscosity $\eta(\dot{\gamma})$ of the 30 wt % BSB/DBP system at 25 °C. At low $\dot{\gamma} < 0.1$ s^{-1}, η is almost proportional to $\dot{\gamma}^{-1}$ and the plastic flow behavior prevails. At high $\dot{\gamma} > 0.1$ s^{-1}, the $\dot{\gamma}$ dependence of η becomes weaker, and the thinning without the plastic character is noted. This thinning behavior suggests that the network is considerably disrupted in this high-shear regime.

This disruption is confirmed in Figure 4 where the SANS profiles of the BSB/DBP system under the steady shear (curves) are compared with the profile at equilibrium (squares). Since the shear affected the $I(q)$ data only at small q around the $I(q)$ peak, a magnified log $I(q)$ vs q plot is shown only at those q. All these profiles were obtained with the same exposure time (10 min) and can be quantitatively compared.

As seen in Figure 4, the position q_1 of the first-order scattering peak does not significantly change with increasing $\dot{\gamma}$/s^{-1} from 0 to 1, but this peak becomes lower by a factor ≅20% on this increase of $\dot{\gamma}$; compare the squares and thick dashed curve. Correspondingly, the first-order peak is broadened (as characterized by an increase of the peak width at the half-maximum from 0.059 to 0.075 nm^{-1}), and the higher-order shoulders

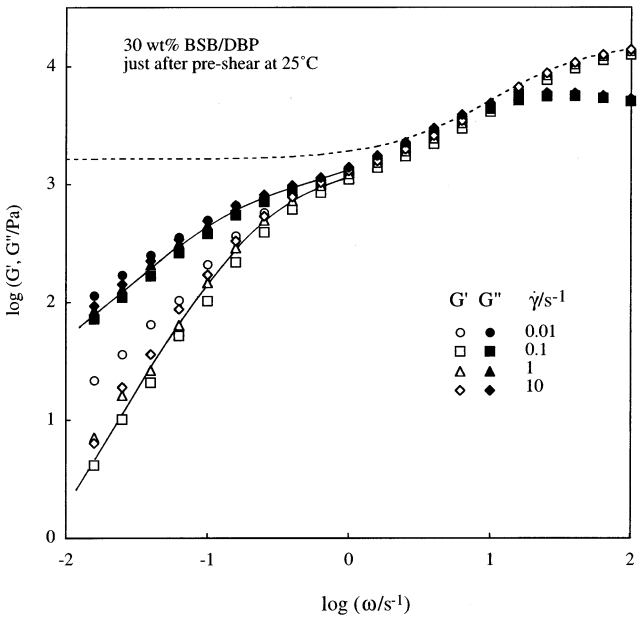

Figure 5. Linear viscoelastic moduli of the 30 wt % BSB/DBP system just after the steady preshear (symbols). The dotted curve indicates the storage modulus at equilibrium.

resolved at equilibrium are smeared into a broad tail with increasing $\dot{\gamma}$ up to 1 s^{-1}. These results indicate that the B domains themselves are preserved under the shear, but their lattice-type network is progressively disrupted as $\dot{\gamma}$ is increased to 1 s^{-1}. However, on a further increase of $\dot{\gamma}$ up to 10 s^{-1}, the $I(q)$ profile becomes closer to that at equilibrium, and the network disruption becomes less significant; see the thin dotted curve. Thus, the network is disrupted in a nonmonotonic way, and the heaviest disruption occurs at an intermediate shear rate, $\dot{\gamma} \cong 1$ s^{-1}.

An origin of this nonmonotonic disruption can be examined through the linear viscoelastic moduli G' and G'' measured just after cessation of the steady shear. As shown in Figure 5, the fast relaxation process of individual BSB chains (seen at $\omega \geq 10$ s^{-1}) is not affected by the shear, while the equilibrium elasticity seen at low ω vanishes immediately after the shear. This presheared BSB/DBP system exhibits the terminal relaxation behavior that is insensitive to the preshear rate in a range of $\dot{\gamma} \geq 0.1$ s^{-1} (where the nonplastic thinning behavior is observed for the η data). This terminal relaxation is expected to be the relaxation of the B/S concentration fluctuation, as was the case for the presheared BS/DBP system.[19] (Note that the concentration fluctuation corresponds to the collective motion of many copolymer chains and is much slower than the relaxation of individual chains.[1,26,27])

The above expectation is tested in Figure 6 where the G' and G'' data at 25 °C obtained for the 30 wt % BSB/DBP system presheared at 1 s^{-1} (filled circles) are compared with the data of the same system fully equilibrated at various T. The data for a slightly less concentrated system ($C_{BSB} = 29$ wt %) at 25 °C, multiplied by a minor factor (=1.03) correcting a difference in the chain number density, are also shown (cf. crosses). In this comparison, the moduli data are plotted against a frequency ωa_T reduced at 25 °C so that differences in the monomeric friction at different T and/or C_{BSB} are compensated. The frequency shift factor a_T was determined in a way that the moduli curves for different T and/or C_{BSB} were superposed at high ω

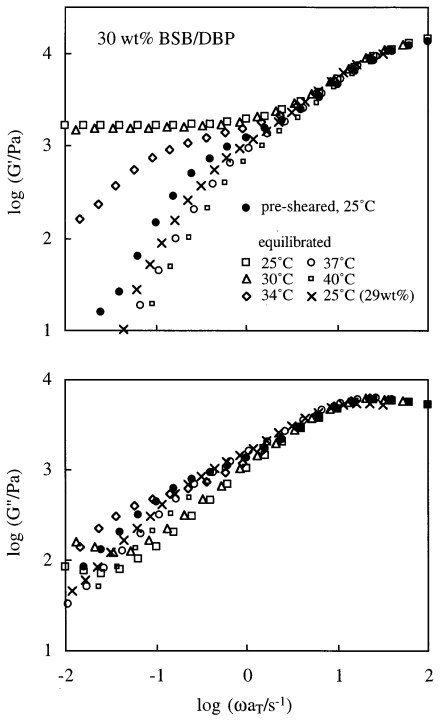

Figure 6. Comparison of the linear viscoelastic moduli measured for the 30 wt % BSB/DBP system at 25 °C just after the preshear at $\dot{\gamma} = 1$ s^{-1}, the same system equilibrated at various T, and the 29 wt % BSB/DBP system equilibrated at 25 °C. The relaxation seen at $\omega a_T \cong 0.4$ s^{-1} is attributable to the B/S concentration fluctuation.

where the relaxation of individual BSB chains was observed. (This type of superposition is often made for comparison of the relaxation behavior of block copolymers in the ordered and disordered states.[1,27])

As noted in Figure 6, the equilibrated 30 wt % BSB system exhibits the order−disorder transition (B/S mixing) at $T \cong 34$ °C, and the slow terminal relaxation in the disordered state at various T (≥37 °C) occurs at roughly the same frequency in the reduced scale, $\omega_f a_T \cong 0.4$ s^{-1}. The disordered 29 wt % BSB system also relaxes at this $\omega_f a_T$. These features, observed also for many copolymer systems in the disordered state,[1,19,26] are characteristic of the relaxation due to the concentration fluctuation. Thus, the terminal relaxation of the presheared 30 wt % BSB/DBP system at 25 °C, occurring at the same $\omega_f a_T$ (cf. filled circles), is attributed to the B/S concentration fluctuation. A similar assignment was made also for the presheared BS/DBP micellar system.[19]

With this assignment, a characteristic frequency ω_f of the B/S concentration fluctuation in the 30 wt % BSB/DBP system at 25 °C was evaluated from the G' and G'' data shown in Figure 5; $\omega_f = [G'/\omega G'']_{\omega \to 0} = 0.4$ s^{-1}. The preshear rate for the heaviest disruption of the lattice-type network in this system, $\dot{\gamma} \cong 1$ s^{-1}, is close to this ω_f. From this result, the heaviest disruption appears to occur when the shear just overwhelms the B/S concentration fluctuation: The fluctuation enables a spatial transfer of BSB chains, thereby repairing the disrupted portion of the network structure. This repairing mechanism is quenched with increasing $\dot{\gamma}$ up to ω_f. At the same time, the defects in the network structure can be aligned in the flow direction at $\dot{\gamma} \gg \omega_f$.[19] For this case, the applied shear tends to be localized in these aligned defects to reduce the magnitude of the shear-induced disruption. Thus, the heaviest disruption possibly occurs at $\dot{\gamma} \cong \omega_f$ (as observed) where neither the repairing mechanism nor the defect-aligning mechanism efficiently works. This situation for the BSB/DBP system is essentially the same as that for the BS/DBP micellar system.[19]

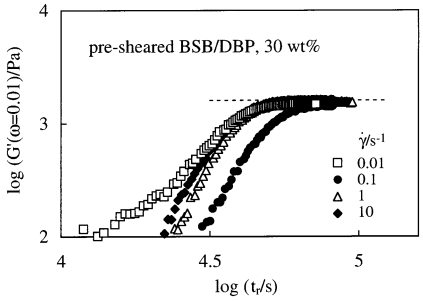

Figure 7. Time-dependent changes of G' ($\omega = 0.01$ s^{-1}) measured for the 30 wt % BSB/DBP system presheared at 25 °C. The horizontal dotted line indicates G_e in the fully equilibrated state.

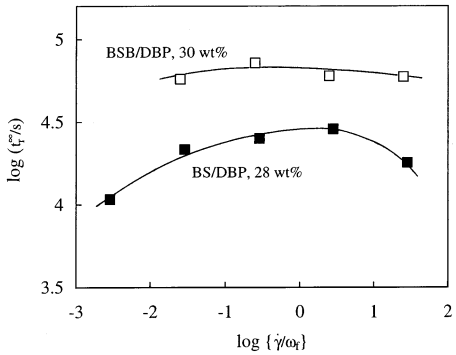

Figure 8. Time t_r^∞ required for full recovery of the equilibrium elasticity of the 30 wt % BSB/DBP and 28 wt % BS/DBP[19] systems presheared at 25 °C. This t_r^∞ is plotted against the preshear rate normalized by the B/S concentration fluctuation frequency, $\dot{\gamma}/\omega_f$, with $\omega_f = 0.4$ and 3.5 s^{-1} for the BSB and BS systems, respectively. In the previous paper, the t_r^∞ values for the BS/DBP system were evaluated from G' at $\omega = 0.1$ s^{-1}.[19] However, no difference was found for the t_r^∞ values reevaluated from G' at $\omega = 0.01$ s^{-1} (the frequency utilized in this paper for the BSB system); cf. Figures 8−10 in ref 19. Thus, the difference in the t_r^∞ data of the BSB and BS systems seen here unequivocally indicates a difference in the elasticity recovery behavior of these systems.

3.3. Recovery of Elasticity after Preshear. For the 30 wt % BSB/DBP system presheared at various $\dot{\gamma}$, Figure 7 shows changes of the low-ω storage modulus $G'(\omega = 0.01$ s$^{-1})$ with a quiescent rest time t_r. After a sufficiently long rest, this modulus is increased to the equilibrium modulus G_e shown with the horizontal dotted line. This G_e is sustained not only by the bridge-type S blocks but also by the loops. Thus, the recovery of the equilibrium elasticity corresponds to a full recovery of the order of the lattice-type network of the B domains: This order is required for the dangling loops to exhibit the elasticity, as explained earlier.

A time t_r^∞ required for the full recovery of the equilibrium elasticity of the BSB/DBP system was evaluated as the t_r where the G' value after the preshear (Figure 7) coincided with the G_e value within 10% (unavoidable uncertainty in the measurement of G' after the shear). Figure 8 shows the t_r^∞ of this system together with the t_r^∞ of the previously examined 28 wt % BS/DBP micellar system, the latter evaluated in the same way. For quantitative comparison of the elasticity

Table 1. Time t_r^∞ for the Full Recovery of the Elasticity for the 30 wt % BSB/DBP and 28 wt % BS/DBP Systems Presheared at 25 °C

preshear rate/s^{-1}	$10^{-4}t_r^\infty$/s
BSB/DBP System	
0.01	5.8
0.1	7.2
1	6.0
10	5.9
BS/DBP System[19]	
0.01	1.1
0.1	2.2
1	2.5
10	2.9
100	1.8

recovery behavior of the BSB and BS systems, the t_r^∞ is double-logarithmically plotted against the preshear rate normalized by the B/S concentration fluctuation frequency, $\dot{\gamma}/\omega_f$. The raw t_r^∞ values of these systems are summarized in Table 1.

The t_r^∞ of the BS system exhibits a distinct peak at $\dot{\gamma} \cong \omega_f$. This peak reflects a quite natural situation that the recovery of the micellar lattice in the BS system is the slowest when the lattice is most heavily disrupted at $\dot{\gamma} \cong \omega_f$.[19] For the BSB system, the heaviest disruption of the lattice-type network occurs also at $\dot{\gamma} \cong \omega_f$ (see Figure 4). Nevertheless, the t_r^∞ of this system depends on $\dot{\gamma}$ much more weakly. Note that the t_r^∞ values of the BSB system obtained for various $\dot{\gamma}$ agree with each other within ±15% (cf. Figures 7 and 8).

This difference between the BSB and BS systems suggests that the full recovery of the elasticity in the former system is governed by a process absent in the latter. This process can be a recovery of the equilibrium population of the bridge-type middle S block, as discussed below.

3.4. Elasticity Recovery Mechanism in the BSB System. In general, defects exist in the microdomain arrangement in block copolymer systems, and the applied deformation tends to be localized in the defect region. In particular, the steady flow would be mostly localized in the flow-created defect plane. Thus, for the BSB/DBP system under steady shear, a large fraction of the S bridges crossing this flow-created defect plane would have been converted into dangling loops.[5−7] (Under the flow, the B blocks anchoring the S bridges can be easily pulled out from the soft, rubbery B domains, thereby allowing this conversion.) Since the domain arrangement is largely disordered across the defect plane, those loops do not sustain the equilibrium elasticity just after cessation of the shear. Correspondingly, the equilibrium modulus G_e vanishes for the BSB system as a whole, because the small strain utilized in the G_e measurement is localized (or absorbed) in the flow-created defect plane.

Thus, the full recovery of the elasticity of the BSB system should occur through the recovery of the well-ordered arrangement of the B domains across the flow-created defect plane (i.e., the order recovery necessary for the appearance of the loop elasticity) and the re-formation of the S bridges connecting the B domains across this plane, as schematically shown in Figure 9.

In Figure 9, an early stage of the elasticity recovery is shown as a process from part a to part b. In this stage, a short-ranged motion of the B domains restricted by the bridges thereon may result in a partial recovery of the order in the domain arrangement *without* significant re-formation of the flow-disrupted bridges. Thus, the

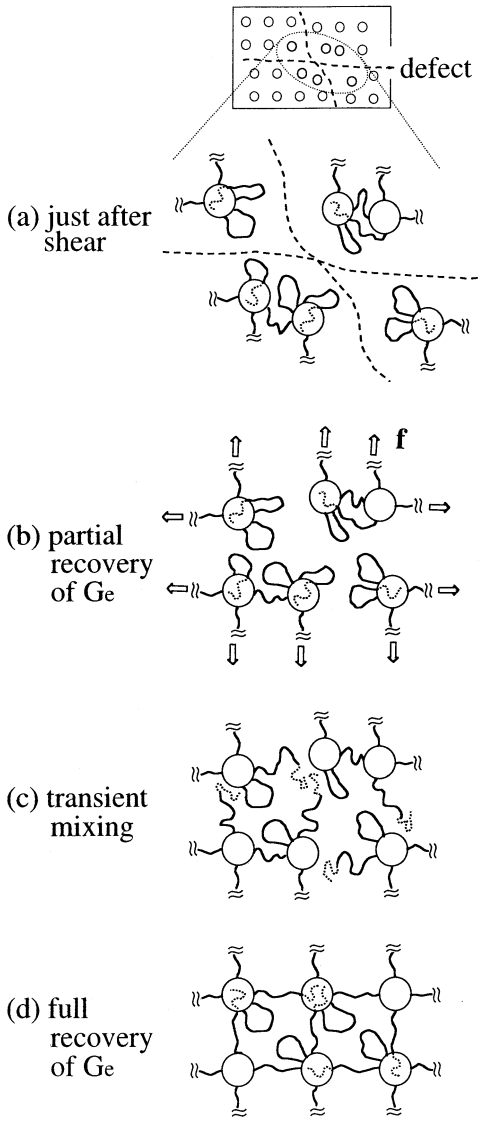

Figure 9. Schematic illustration of the elasticity recovery process of the presheared BSB/DBP system. Just after the shear (part a), the bridges crossing the flow-created defect planes are converted to the dangling loops. Because of the lack of the network connectivity and the order of the B domain arrangement in the defect region, the S bridges/loops exhibit no elasticity just after the preshear. After a short-ranged motion of the B domains restricted by the nondisrupted bridges thereon (part b), the order of the domain arrangement near the defect plane may be partially recovered *without* significant reformation of the flow-disrupted bridges. The tension **f** of these bridges (arrows) tends to keep the B domains away from the defect plane, thereby disturbing a close approach of the domains across this plane, i.e., the motion required for the full recovery of the order. This full recovery (part d) is achieved through the re-formation of the bridges across the defect plane; the re-formed bridges give a tension balancing with the tension **f** of the nondisrupted bridges and pulling the B domains toward the defect plane, thereby enabling this approach. This bridge re-formation occurs through the entropically driven migration of the B blocks associated with the transient mixing of the B and S blocks (part c).

elasticity recovery rate *in the early stage* may be smaller for a more heavily disrupted network and thus depend on $\dot{\gamma}$ (as similar to the situation seen for t_r^∞ of the BS/DBP micellar system). In fact, Figure 7 demonstrates that a time t_r^{fr} required for G' of the presheared BSB system to increase up to a *small fraction* of the G_e value considerably changes with $\dot{\gamma}$; for example, t_r^{fr} for the

increase of G' up to 100 Pa ($=0.063G_e$) changes by a factor of $\pm 60\%$ in the range of $\dot{\gamma}$ examined, and this change is much larger than the change (within $\pm 15\%$) seen for the full recovery time t_r^{∞}. Note also that the t_r^{fr} value is larger for $\dot{\gamma} = 0.1-1\ s^{-1}$ (where the lattice is strongly disrupted) than for $\dot{\gamma} = 0.01$ and $10\ s^{-1}$.

In a late stage for the full recovery of elasticity shown in Figure 9 as a process from part b to part d, the B domains across the flow-created defect plane need to fully recover the order in their arrangement so that the dangling S loops (as well as the S bridges) exhibit the equilibrium elasticity. The bridges crossing the defect plane, converted into the loops during the preshear, have not been re-formed just after the early stage, and the B domains are subjected to the tension **f** from the bridges not crossing this plane and preserved under the preshear (cf. arrows in Figure 9b). This tension tends to keep the B domains away from the defect plane and disturb a close approach of the domains across this plane, the motion necessary for the order recovery. Thus, the order recovery requires the re-formation of the bridges crossing the defect plane; these re-formed bridges give the tension pulling the B domains toward the defect plane and allow this approach. In other words, the re-formed bridges stitch up the flow-created defect plane to allow the recovery of the dangling loop elasticity (i.e., the full recovery of the elasticity of the system as a whole; cf. Figure 9d).

For this bridge re-formation to occur during the quiescent rest, a B block needs to *thermally* escape from its domain and migrate to the other B domain across the flow-created defect plane. This entropically driven migration is associated with a thermodynamically unfavorable, transient mixing of the S and B blocks (see Figure 9c). Thus, the rate of the bridge re-formation would be essentially determined by the S/B mixing enthalpy being insensitive to the preshear rate $\dot{\gamma}$. This $\dot{\gamma}$ insensitivity appears to result in the observed, very weak $\dot{\gamma}$ dependence of the time t_r^{∞} for the full recovery of the elasticity in the BSB system (Figure 8).

Concerning this argument, we have to emphasize that the S bridges should exhibit the elasticity whenever the network of these bridges are connected throughout the system and the applied strain is effectively transmitted to individual bridges[10] (as usually considered in the rubber elasticity theory). In other words, the bridge elasticity *can* emerge even when the B domains have no order in their arrangement. From this point of view, the bridge elasticity is different from the dangling loop elasticity: As explained earlier, the dangling loop elasticity emerges only when this order exists and the applied strain effectively distorts the loop conformation under the osmotic constraint. However, for the BSB system just after the preshear, the network connectivity is broken at the shear-created defect plane to hide the elasticity of the preserved bridges (cf. Figure 9a), and the re-formation of the bridges across this plane leads to the recovery of both of the network connectivity and the order of the B domain arrangement. In this sense, the bridges and loops appear to fully recover their elasticity simultaneously through the bridge re-formation process.

Finally, we note that the transient B/S mixing required for the full recovery of the elasticity in the presheared BSB system is intimately related to diffusion[28] and plastic flow[7,9] in lattice-type network systems of microphase-separated triblock copolymers. The diffusion of copolymer chains also occurs through the transient mixing of the end and middle blocks; the diffusion coefficient drastically decreases with an increase of the mixing enthalpy (or mixing energy),[28] and the yield stress of the triblock network system in a strongly segregated state is determined by this enthalpy.[7,9] Specifically, for 2-vinylpyridine−styrene−2-vinylpyridine (PSP) triblock copolymers, Yokoyama and Kramer[28] observed an exponential dependence of the diffusion coefficient D on $-\chi_{P-S}N_P$, where χ_{P-S} is the interaction parameter between P and S blocks and N_P is the polymerization index of the end P blocks. Furthermore, they found two characteristic dependencies, $D \propto \exp(-\chi_{P-S}N_P)$ for large $\chi_{P-S}N_P$ (≥ 10) and $D \propto \exp(-2\chi_{P-S}N_P)$ for relatively small $\chi_{P-S}N_P$: The former type of dependency was attributed to a "walking diffusion" activated by the thermal escape of one end block from its domain, and the latter was assigned to a "double activation diffusion" resulting from simultaneous escape of the two end blocks.

It is of interest to test whether the elasticity recovery time t_r^{∞} in our BSB/DBP system is directly related to the walking and/or double activation diffusion processes. Unfortunately, the data of the χ parameter between the B and S blocks in our system and the diffusion coefficient D_0 of the BSB chain in the mixed state, both being required for this test, are not available. However, we note that the $t_r^{\infty} = (6.5 \pm 0.7) \times 10^4$ s (Figure 8) is significantly larger than the relaxation time of individual chains, $\tau_{chain} = 1/\omega_{chain} \cong 0.1$ s (cf. Figure 5). This large difference might be related to an exponential decrease of D with χN: Regarding the $t_r^{\infty}/\tau_{chain}$ ratio to be close to the diffusion coefficient ratio, $D_0/D \cong \exp(2\chi N)$ for $\chi N < 10$,[28] we estimated a χN value giving the $t_r^{\infty}/\tau_{chain}$ ratio ($\cong 6.5 \times 10^5$). It turned out that a reasonable value of χN ($=6.7$) gives this large $t_r^{\infty}/\tau_{chain}$ ratio.[24]

4. Concluding Remarks

For the BSB triblock copolymer in the S-selective solvent, DBP, we have examined the shear effects on the rheological and structural properties. The bcc lattice-type network of the B domains connected by the S bridges, formed at equilibrium, was disrupted under the steady shear to various magnitudes, and the heaviest disruption occurred at the shear rate $\dot{\gamma}$ close to the frequency of the B/S concentration fluctuation ω_f. This disruption behavior is similar to that seen for the micellar lattice of the BS diblock copolymer (a half-fragment of BSB).

However, a difference between the BSB/DBP and BS/DBP systems was noted for the time t_r^{∞} required for the full recovery of the equilibrium elasticity after cessation of the steady shear. The t_r^{∞} of the BS system was strongly dependent on $\dot{\gamma}$, and the maximum t_r^{∞} value was observed for $\dot{\gamma} \cong \omega_f$ (where the micellar lattice was most heavily disrupted). In contrast, the t_r^{∞} of the BSB system changed with $\dot{\gamma}$ much more weakly, despite a fact that the magnitude of the network disruption significantly changed with $\dot{\gamma}$. This recovery behavior of the BSB system can be related to the re-formation of the bridges from the flow-created dangling loops, a process absent in the BS system. This bridge re-formation is associated with a thermodynamically unfavorable, transient B/S mixing. Thus, the re-formation rate appears to be determined by the $\dot{\gamma}$-insensitive mixing enthalpy. This $\dot{\gamma}$ insensitivity possibly leads to

the observed, very weak $\dot{\gamma}$ dependence of the t_r^∞ of the BSB system.

Acknowledgment. This work was partly supported by the Ministry of Education, Culture, and Sports, Science, and Technology, Japan (Grant 13450391). H.T. gratefully acknowledges the Jinnai scholarship provided by Association of International Education, Japan.

References and Notes

(1) Watanabe, H. Rheology of Multiphase Polymeric Systems. In Araki, T., Qui, T. C., Shibayama, M., Eds.; *Structure and Properties of Multiphase Polymeric Materials*; Marcel Dekker: New York, 1998; Chapter 9.
(2) Chung, C. I.; Gale, J. C. *J. Polym. Sci., Phys. Ed.* **1976**, *14*, 1149.
(3) Gouinlock, E. V.; Porter, R. S. *Polym. Eng. Sci.* **1977**, *17*, 535.
(4) Pico, E. R.; Williams, M. C. *Polym. Eng. Sci.* **1977**, *17*, 573.
(5) Morrison, F. A.; Winter, H. *Macromolecules* **1989**, *22*, 3533.
(6) Morrison, F. A.; Winter, H.; Gronski, W.; Barnes, J. D. *Macromolecules* **1990**, *23*, 4200.
(7) Watanabe, H.; Kuwahara, S.; Kotaka, T. *J. Rheol.* **1984**, *28*, 393.
(8) Sato, T.; Watanabe, H.; Osaki, K. *Macromolecules* **1996**, *29*, 6231.
(9) Watanabe, H.; Sato, T.; Osaki, K.; Yao, M. L.; Yamagishi, A. *Macromolecules* **1997**, *30*, 5877.
(10) Watanabe, H.; Sato, T.; Osaki, K. *Macromolecules* **2000**, *33*, 2545.
(11) Hamley, I. W.; Fairclough, J. P. A.; Ryan, A. J.; Ryu, C. Y.; Lodge, T. P.; Gleeson, A. J.; Pedersen, J. S. *Macromolecules* **1998**, *31*, 1188.
(12) Spontak, R. J.; Wilder, E. A.; Smith, S. D. *Langmuir* **2001**, *17*, 2294.
(13) Laurer, J. H.; Khan, S. A.; Spontak, R. J.; Satkowski, M. M.; Grothaus, J. T.; Smith, S. D.; Lin, J. S. *Langmuir* **1999**, *15*, 7947.
(14) Watanabe, H.; Kotaka, T.; Hashimoto, T.; Shibayama, M.; Kawai, H. *J. Rheol.* **1982**, *26*, 153.
(15) Watanabe, H.; Kotaka, T. *J. Rheol.* **1983**, *27*, 223.
(16) Watanabe, H. *Acta Polym.* **1997**, *48*, 215.
(17) Watanabe, H.; Kanaya, T.; Takahashi, Y. *Macromolecules* **2001**, *34*, 662.
(18) McConnell, G. A.; Lin, M. Y.; Gast, A. P. *Macromolecules* **1995**, *28*, 6754.
(19) Watanabe, H.; Matsumiya, Y.; Kanaya, T.; Takahashi, T. *Macromolecules* **2001**, *34*, 6742.
(20) Lodge, T. P.; Xu, X.; Ryu, C. Y.; Hamley, I. W.; Fairclough, J. P. A.; Ryan, A. J.; Pedersen, J. S. *Macromolecules* **1996**, *29*, 5955.
(21) Hanley, K. J.; Lodge, T. P.; Huang, C. I. *Macromolecules* **2000**, *33*, 5918.
(22) Ferry, J. D. *Viscoelastic Properties of Polymers*, 3rd ed.; Wiley: New York, 1980.
(23) Takahashi, Y.; Noda, M.; Naruse, M.; Kanaya, T.; Watanabe, H.; Kato, T.; Imai, M.; Matsushita, Y. *J. Soc. Rheol. Jpn.* **2000**, *28*, 187.
(24) Even in the fully equilibrated state, the entropically driven migration of the B blocks would occur through the transient B/S mixing in a time scale of $t_r^\infty \cong 6.5 \times 10^4$ s (Figure 8). The slow, partial relaxation seen for the equilibrated BSB system at $\omega \ll 0.01$ s^{-1} (Figure 1) may correspond to this migration. However, a *simultaneous* migration of many B blocks belonging to the same B domain, a process required for the full relaxation of the system, should be tremendously slower than the migration of one B block and would not occur in detectable time scales. Thus, *in a practical sense*, the BSB/DBP system having the equilibrated lattice-type network structure exhibits a static elasticity (associated with an infinitely long terminal relaxation time).
(25) Hashimoto, T.; Shibayama, M.; Kawai, H. *Macromolecules* **1980**, *13*, 1237.
(26) Bates, F. S.; Rosedale, J. H.; Fredrickson, G. H. *J. Chem. Phys.* **1990**, *92*, 6255.
(27) Bates, F. S.; Fredrickson, G. H. *Annu. Rev. Phys. Chem.* **1990**, *41*, 525.
(28) Yokoyama, H.; Kramer, E. *Macromolecules* **2000**, *33*, 954.

MA021654Q